Inorg. Chem. **2008**, *47*, 8613−8615

In Situ Crystallography of $KHSO_4$: Probing the Kinetic Pathway for the Evolution of a Pyrolysis Reaction in the Crystalline State

Diptikanta Swain and Tayur N. Guru Row*

Solid State and Structural Chemistry Unit, Indian Institute of Science (IISc), Bangalore 560012, India

Received July 30, 2008

Variable-temperature in situ crystallography on $KHSO_4$ shows that the pyrolysis of $KHSO_4$ to $K_2S_2O_7$ occurs via a three-step kinetic pathway monitored by crystal-to-crystal phase transitions while providing an explanation for the high proton conductivity to be due to the disordered hydrogen-bonding pattern.

The phase transition of $KHSO_4$ with temperature has been studied extensively[1−8] but has never been fully understood. The conflicting results obtained from structural, thermal, and spectroscopic studies suggest that there are some anomalies in modeling the phase-transition pathways. High-pressure studies on $KHSO_4$ suggested the possibility of its decomposition to $K_3H(SO_4)_2$ at pressures above 1.5 GPa with the elimination of H_2SO_4.[9] Conductivity measurements provide the signature of a fast proton conductance[10] at 468 K, and the mechanism is explained to be due to distortions in the HSO_4^- ion, resulting in the disruption of a hydrogen-bonded network. In our attempts to study the structural phase transitions using in situ crystallography, we have found a remarkable kinetic pathway leading to an understanding of the changes in the hydrogen-bonding patterns steering toward the final pyrolysis reaction product, $K_2S_2O_7$. In the following, we report the evolution of a kinetically driven pathway across three transitions at 463, 475, and 485 K and describe the structural features. It is of interest to note that the observations reported here could be made only with in situ crystallography with controlled heating with a slow ramp rate of 30 K/h.

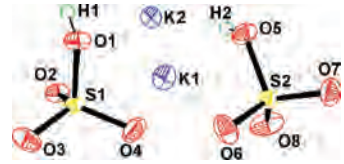

Figure 1. ORTEP diagram showing the asymmetric unit contents.

The crystal was mounted inside an open-ended Lindemann glass capillary. X-ray diffraction data were collected on a Bruker AXS SMART APEX CCD diffractometer. The X-ray generator was operated at 50 kV and 40 mA using Mo Kα radiation. For all of the measurements, 606 frames per set were collected using *SMART*[11] in four different settings of φ (0°, 90°, 180°, and 270°) with an ω scan at −0.3° intervals and with a counting time of 15 s, while keeping the sample-to-detector distance at 6.054 cm and 2θ value fixed at −25°. The data were processed using *SAINT-PLUS*[11] protocol, and an empirical absorption correction was applied using the package *SADABS*[12] followed by *XPREP*[11] to determine the space group. The structures were solved and refined using the *SHELX-97*[13] program present in the *WinGX*[14] suite. The conventional R factor, the weighted R factor wR, and the goodness of fit S are based on F^2. The threshold expression of $F^2 > 2\sigma(F^2)$ is used only for calculation of the R factor and is not relevant to the choice of reflections for refinements. In situ high-temperature measurement was carried out with an attached OXFORD cryosystem, maintaining a heating rate of 30 K/h by using a temperature controller with liquid-N_2 flow.

The structure of $KHSO_4$ determined at room temperature confirms the details of the earlier report[3,15] and belongs to the orthorhombic system, space group *Pbca* with $Z = 16$ (Figure 1). There is an extensive hydrogen-bonded network, with the two crystallographically independent HSO_4^- ions

* To whom correspondence should be addressed. E-mail: ssctng@sscu.iisc.ernet.in.

(1) Rogrs, S. E.; Ubbelohde, A. R. *Trans. Faraday Soc.* **1950**, *46*, 1051.
(2) Bridgman, P. W. *Am. Acad. Arts Sci.* **1916/1917**, *52*, 9.
(3) Payan, F.; Haser, R. *Acta Crystallogr.* **1976**, *B32*, 1875.
(4) Cotton, F. A.; Foemz, B. A.; Hunter, D. L. *Acta Crystallogr.* **1975**, *B31*, 302.
(5) Sharon, M.; Kalia, A. K. *J. Chem. Phys.* **1977**, *66*, 3051.
(6) Kandil, S. H.; Kassem, M. E.; Abd El-Rehim, M.; Bayoumi, A. M. *Thermochim. Acta* **1988**, *132*, 1.
(7) Diosa, J. E.; Vargas, R. A.; Mina, E.; Torijano, E.; Mellander, B.-E. *Phys. Status Solidi* **2000**, *b220*, 641.
(8) Gerlich, D.; Siegert, H. *Acta Crystallogr.* **1975**, *A31*, 207.
(9) Bagdassarov, N.; Lentzb, G. *Solid State Commun.* **2005**, *136*, 16.
(10) Kassem, M. E. *J. Therm. Anal.* **1991**, *37*, 513.
(11) *SMART, SAINT, SADABAS, XPREP, and SHELXTL*; Bruker AXS Inc.: Madison, WI, 1998.
(12) Sheldrick, G. M. *SADABS*; University of Göttingen: Göttingen, Germany, 1996.
(13) Sheldrick, G. M. *SHELXL97, program for crystal structure refinement*; University of Göttingen: Göttingen, Germany, 1997.
(14) Farrugia, L. J. *J. Appl. Crystallogr.* **1999**, *32*, 837.
(15) Loopstra, L. H.; Macgillavry, C. H. *Acta Crystallogr.* **1958**, *11*, 349.

10.1021/ic801426f CCC: $40.75
Published on Web 09/09/2008

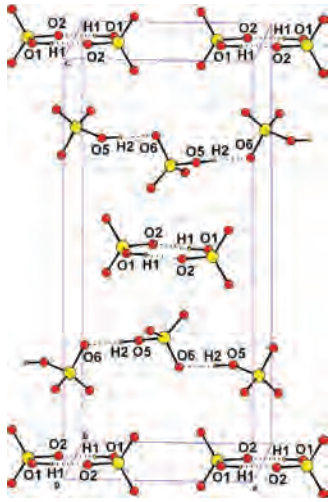

Figure 2. Hydrogen-bonding scheme showing layers of dimers and polymeric chains of $KHSO_4$ at 293 K.

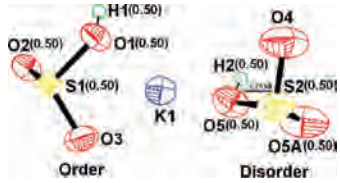

Figure 3. ORTEP diagram showing asymmetric unit contents.

forming both dimeric and chain structures.[16] In fact, the hydrogen-bonded dimers are formed across the center of symmetry with an O···O distance of 2.518(2) Å, and the glide plane generates hydrogen-bonded chains along the *a* axis with an O···O distance of 2.620(2) Å (Figure 2).

Upon heating to 463 K in situ on a single-crystal X-ray diffractometer at a ramp rate of 30 K/h, keeping the temperature steady for 2 h and checking the CCD images at regular intervals, we observed a structural phase transition to a space group *Bbcm*, with $Z = 16$.[17] The two S atoms occupy special positions, one at mirror symmetry and the other at the 2-fold symmetry axis (Figure 3; also see the Supporting Information). The coordination around the K atom remains the same; however, the structure is disordered at O and H sites, and one of the S−O bond distances becomes 1.753(4) Å. The hydrogen-bonding features at high temperature remain similar to those in the room temperature structure, infinite polymeric chains as well as zero-dimensional dimers (Figure 4).

The hydrogen-bonding features at high temperature remain similar to those in the room temperature structure, infinite polymeric chains as well as zero-dimensional dimers (Figure 4). The long S−O bond is a consequence of the disorder at atom O(5) and its corresponding H. This also suggests that

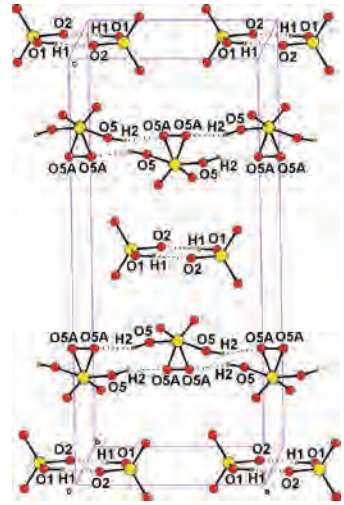

Figure 4. Hydrogen-bonding scheme showing ordered dimers and disordered polymeric chains of $KHSO_4$ at 463 K.

there is a possibility of disruption of the polymeric hydrogen bond. It is of interest to note that these structural changes correlate with the earlier observations made with respect to electrical conductivity and variable-temperature NMR studies.[18] It was also suggested that the rather high conductivity of 10^{-1} S/cm is due to the hopping of protons. In another article,[19] there was a suggestion that the proton conduction mechanism in $KHSO_4$ is due to the conversion of dimer into polymeric chains and a synchronized rotation of the hydrogen-bonding chain. Our studies clearly suggest the contrary, that the structural phase transition results from disorder due to the additional symmetry associated with the HSO_4^- moiety in the polymeric hydrogen-bonded chain. The expected pathway for this phase transition is given as follows:

$$2KHSO_4(O) \xrightarrow{463\ K} KHSO_4(O) + KHSO_4(D)$$

$$O = \text{order}, \quad D = \text{disorder}$$

In order to check this hypothesis further, we continued heating and, reaching 475 K and keeping the capillary for 2 h at this temperature, observed yet another structural change. The structure now is monoclinic, $P2_1/c$, with the formula unit $K_3HS_3O_{11}$ (representing $KHSO_4 \cdot K_2S_2O_7$).[20]

Figures 5 and 6 represent the asymmetric unit and the hydrogen-bonding scheme in this phase. We infer that the mechanism of formation of this phase is due to the combination of two disordered units of $KHSO_4$ forming the polymeric chain in the *Bbcm* phase to form $K_2S_2O_7$ with the release of a water molecule, keeping the ordered dimeric $KHSO_4$ intact.

This remarkable observation represents a pyrolysis reaction in the crystalline state, leading to a crystal-to-crystal transition, and to our knowledge, this is the first ever observation

(16) Crystal data: chemical formula $KHSO_4$, fw = 136.18, orthorhombic, space group *Pbca*, $a = 8.415(7)$ Å, $b = 9.796(8)$ Å, $c = 18.967(2)$ Å, $V = 1563.5(2)$ Å^3, $Z = 16$, $\rho_{calc} = 2.314$ g/cm^3, $T = 293$ K, $\mu = 1.753$, reflcn measd = 16 689, unique reflcn = 1886, obsd [$I > 2\sigma(I)$] = 1777, $R[F^2 > 2\sigma(F^2)] = 0.0211$, $wR(F^2) = 0.0550$.

(17) Crystal data: chemical formula $KHSO_4$, fw = 136.18, orthorhombic, space group *Bbcm*, $a = 8.429(1)$ Å, $b = 9.894(1)$ Å, $c = 19.195(2)$ Å, $V = 1600.8(3)$ Å^3, $Z = 16$, $\rho_{calc} = 2.260$ g/cm^3, $T = 463$ K, $\mu = 1.712$, refln measd = 8665, unique reflcn = 1000, obsd [$I > 2\sigma(I)$] = 902, $R[F^2 > 2\sigma(F^2)] = 0.0313$, $wR(F^2) = 0.0794$.

(18) Yoshida, Y.; Matsuo, Y.; Ikehata, S. *Ferroelectrics* **2004**, *302*, 85.

(19) Sharon, M.; Kalia, A. K. *J. Solid State Chem.* **1980**, *31*, 295.

(20) Crystal data: chemical formula $KHSO_4 \cdot K_2S_2O_7$, fw = 390.52, monoclinic, space group $P2_1/c$, $a = 13.473(2)$ Å, $b = 8.165(7)$ Å, $c = 9.811(8)$ Å, $\beta = 97.09(2)°$, $V = 1071.1(13)$ Å^3, $Z = 4$, $\rho_{calc} = 2.422$ g/cm^3, $T = 475$ K, $\mu = 1.906$, reflcn measd = 9152, unique reflcn = 2560, obsd [$I > 2\sigma(I)$] = 1391, $R[F^2 > 2\sigma(F^2)] = 0.0550$, $wR(F^2) = 0.1231$.

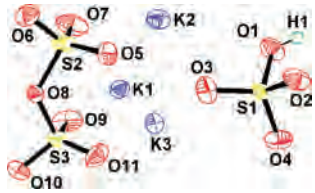

Figure 5. ORTEP diagram showing the asymmetric unit contents.

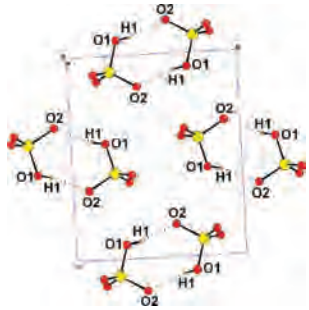

Figure 6. Hydrogen-bonding scheme showing the packing of the dimeric units only of $KHSO_4 \cdot K_2S_2O_7$ at 475 K.

Figure 7. ORTEP diagram showing the asymmetric unit contents.

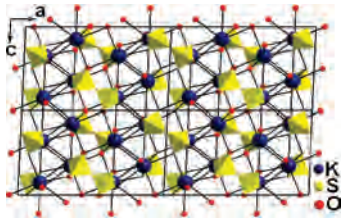

Figure 8. Packing diagram of $K_2S_2O_7$ at 485 K.

of this kind. The coordination of K^+ remains unaltered. The pyrolysis reaction pathway may be represented as follows:

$$KHSO_4(O) + 2KHSO_4(D) \xrightarrow{475\ K} KHSO_4(O) + K_2S_2O_7 + H_2O\uparrow$$

Upon further heating of the crystal to 485 K and keeping the capillary at that temperature for 2 h, the diffraction images can be indexed in a monoclinic system, space group $C2/c$[21] (Figure 7), as reported earlier.[22] The resulting structure is $K_2S_2O_7$. It is to be noted that at 485 K the remaining two ordered units of $KHSO_4$ combine and lose another molecule of water to yield a pyrolysis product $K_2S_2O_7$. The reaction pathway is as follows:

$$KHSO_4(O) + K_2S_2O_7 \xrightarrow{485\ K} 2K_2S_2O_7 + H_2O\uparrow$$

We believe that in situ crystallography opens up the possibility of capturing the dynamics of structural phase transitions and the heating and/or cooling rates would freeze the intermediate kinetically stable forms and allow for structural characterization. The ramp rate of 30 K/h and keeping the crystal at the transition temperature for at least 2 h provide the recipe for stabilization of intermediate phases. The work done earlier and the recognition of fast proton conduction[18,19] in $KHSO_4$ can now be explained on the basis of elongation of one of the S−O bonds associated with the polymeric hydrogen-bonded chain. The subsequent disorder that eventually leads to the *Bbcm* phase is responsible for fast proton conduction because the H atoms now are labile and freely move through the hydrogen-bonded chain, whereas the dimeric motifs keep their identity. It may be conjectured that the two intermediate phases that we have analyzed in the temperature gradient pathway are kinetically stabilized, while the final phase at 485 K is thermodynamically stable. The formation of the intermediate $P2_1/c$ is the key step in the progress of the pyrolysis kinetic pathway.

We conclude that the observation of a kinetic pathway via a crystal-to-crystal transition is unique and provides an explanation for the pyrolysis reaction of $KHSO_4$ to $K_2S_2O_7$ as a three-step process. This further describes the reasons for fast proton conduction, and it may be inferred that such systems will have a major industrial impact in the near future.

Acknowledgment. We thank Department of Science and Technology for funding and IRPHA-DST for the X-ray facility in IISc. D.S. thanks IISc for a senior research fellowship.

Supporting Information Available: Packing diagrams, HKL plots, fractional atomic coordinates, bond lengths, bond angles, and CIF files for all four structures. This material is available free of charge via the Internet at http://pubs.acs.org.

IC801426F

(21) Crystal data: chemical formula $K_2S_2O_7$, fw = 254.34, monoclinic, space group $C2/c$, a = 12.454(2) Å, b = 7.326(1) Å, c = 7.299(1) Å, β = 92.65(3)°, V = 665.13(17) Å^3, Z = 4, ρ_{calc} = 2.540 g/cm^3, T = 485 K, μ = 2.040, reflcn measd = 3190, unique reflcn = 742, obsd [$I > 2\sigma(I)$] = 405, $R[F^2 > 2\sigma(F^2)]$ = 0.0956, w$R(F^2)$ = 0.1182.

(22) Ståhl, K.; Balic-Zunic, T.; da Silva, F.; Eriksen, K. M.; Berg, R. W.; Fehrmann, R. *J. Solid State Chem.* **2005**, *178*, 1697.